

Engine Oil- Crankshaft Interaction Fem Modelling of an Air Cooled Diesel Engine Under Dynamic Severe Functioning Conditions

ABSTRACT

Taking into account the interaction between the engine oil and the crankshaft to model crankshaft thermomechanical behavior under dynamic loading is very important. In particular when the crankshaft is working in severe conditions. This paper deals with an air cooled direct injection-type engine crankshaft thermomechanical FEM modelling accounting for engine oil-crankshaft interaction in severe working conditions. As a case of application we consider the diesel engine Deutz F8L413. The model takes into account 2 forced convective heat fluxes: engine oil and crankcase air. The severe mechanical and thermal characteristics of the engine are experimentally measured on a bench test equipped with a hydraulic brake. The temperature distribution inside the crankshaft was computed using the measured temperature as boundary conditions. The most thermo-mechanical stressed zones of the crankshaft have been determined. The fatigue resistance of the crankshaft under thermo-mechanical conditions was examined using Dang-Van multi-axial fatigue criteria. To prove our model efficiency we have compared crankshaft damage in service to the numerical simulation results. It was found that the breakage occurred in an area where the numerical simulations give the highest stresses.

Keywords: Crankshaft, thermo-mechanic, dynamic behavior, fatigue resistance, severe working, interaction.

1. INTRODUCTION

The automotive crankshafts are working under severe thermo-mechanical conditions. The engine oil in forced convection with crankshaft air transports a significant heat

flux to the crankshaft crankpin and crankshaft bearings. This interaction is very important and requires to be taken into account to deal with the crankshaft thermo-mechanical problem under dynamic loading. This

kind of study is seldom documented in the open literature. In the case of engines with cylinders in V-type, this interaction can produce several thermal effects and merit to be clearly identified in particular for regimes corresponding to maximum power and torque. This work aims to provide a response to this problematic. Several studies concerning the automotive engine thermo-mechanical modelling exist in the literature, as the experimental and analytical study of heat transfer in an engine exhaust port carried out in (Caton and Heywood 1981). (Jarrier et al., 2000) model the effect of engine oil and weather temperature increase to warm the passengers compartment. A new method for determining the heat transfer coefficient for internal combustion engines was introduced by (Woschni, 1967). (Niccoli et al., 2015) developed a thermomechanical model able to simulate the mechanical response of a shape memory alloy heat engine. (Patilet et al., 2015) performed a thermo-mechanical analysis of crankcase in which they coupled crankshaft structural dynamics, the main bearing hydrodynamic lubrication and the engine block stiffness using a system approach. Under 3D modelling, (Menget et al., 2011) proceeded the modal analysis of a 4-cylinder crankshaft using

finite elements method. A simulation of crankshaft dynamic behavior of engine with cylinders in V type was performed in (Niino et al., 1992) by measuring experimentally using gauge stress amplitude at the crankpins for high and low engine speed. A fatigue analysis and life estimation of crankshaft is performed in (Metkare et al., 2011). A crankshaft system modelling for structural dynamic analysis of internal combustion engines is performed in (Mourelatos, 2001). However, crankshaft thermo-mechanical modelling account for the engine oil-crankshaft interaction in severe working conditions is seldom addressed, especially on engines with cylinders in V-type under maximum loading conditions (regime of maximum power and torque). In addition, the few thermo-mechanical models of crankshaft found in the literature seem more interested in the overall look of the set of crankcase-crankshaft thermal response.

In this paper we investigate the crankshaft thermomechanical modelling account for the engine oil crankshaft interaction effects in severe dynamic working conditions, which are deduced from experimental measurements on bench. The engine oil temperature at maximum regimes are obtained through thermocouple measurements. As case study, Deutz

diesel engine types F8L413 with four (4) crankpins to 90 widely spread is considered. The mechanical behavior in dynamic of the same engine is performed in (Keita et al.,2014), in this work we investigate the thermo-mechanical analysis taking into account the engine oil-crankshaft interaction in order to simulate the global thermo-mechanical behavior under severe dynamic working conditions. The heat convective flux of the engine oil and crankcase air are considered in interaction with the crankshaft.

The main contribution of this work is that thanks to experimental measurement of the engine oil in engine real working conditions, we proper model the engine oil-crankshaft interaction problem to

analyze the global 3D thermo-mechanical behavior of the crankshaft. This paper is organized as follows. First, the experimental results are briefly recalled, the details can be found in (Keita et al.,2014). It is followed by the engine oil temperature measurement presentation. Then engine oil-crankshaft interaction model is presented as well as the 3D finite element modelling of the crankshaft. At the end step, the thermo-mechanical simulations are carried out in the permanent and dynamic regimes. The simulation results and post-processing are presented. The thermo-mechanical fatigue analysis is performed. At the end, crankshaft damage in service is compared to the numerical simulations, the model shows a good agreement.

2. METHODOLOGY

2.1. CRANKSHAFT THERMAL MODELLING

In this model we specially consider thermal effects due to the convective heat flux of the engine oil and crankcase air which are transported on the crankshaft. The engine oil and crankcase air being in forced convection, their motions are supposed to be laminar and turbulent respectively for the engine oil and crankcase air. We also

assume the reciprocating movement of the crankpin and crankshaft bearing does not change the engine oil laminar regime. In severe functioning state (regime of maximum power and torque), between the engine oil and crankpin, the heat flux density can be expressed by the following equation:

$$q = h_{oil\text{crankpin}} (T - T_{oil}) n \quad (1)$$

Where q , is the heat flux density n , the unit normal vector T , the

temperature of the crankshaft and T_{oil} , the engine oil temperature and $h_{oilcrapin}$ the convection coefficient of the engine oil. Similarly, between the engine oil and the crankshaft bearing, the heat flux density is expressed in the same manner (equation (2))

$$q = h_{oilbearing} (T - T_{oil}) n \quad (2)$$

Where $h_{oilbearing}$, is the engine oil-crankshaft bearing convection coefficient. In also, between the crankcase air and flyweights and

2.2. ENGINE OIL- CRANKSHAFT INTERACTION MODELLING

In this section we determine the convection coefficients $h_{oilcrapin}$ and $h_{oilbearing}$. For that purpose, the engine oil motion is assumed to be in laminar flow between two horizontal and parallel plates in relatively movement (Couette type flow) that constitute the bearing bush and the crankpin. Then the coefficient $h_{oilcrapin}$ can be calculated. While the coefficient $h_{oilbearing}$ is calculated by assumed the hydrodynamic bearing model (see Keita et al., 2014). Figure 1

$$\overline{Nu}_u = \frac{h_{oilbearing} D_e}{\lambda} \quad (4)$$

With $De = 2e$

arms there is an out coming heat flux density which is the following:

$$q = h_{air} (T - T_{air}) n \quad (3)$$

In equation (3), h_{air} represents the crankcase air convection coefficient. In our model, the convection coefficients $h_{oilcrapin}$ and $h_{oilbearing}$ will be determined by assuming the flow laminar of engine oil between two horizontal and parallel fixed plates that constitute the crankpins and bush as we will detail in the next section.

represents the calculation scheme of the convections coefficients. As discussed before, the flow of the engine oil in the above two cases can be assumed laminar between two horizontal and parallel fixed plates. In this case a mean value of Nusselt number can be estimate independently of Reynolds number (Atkinson et al., 1969 and Huetzet al). This value is $Nu = 4$.

On the other hand, the Nusselt number is expressed as

Where e , is the lubricant film thickness (Figure 1), λ represents the thermal conductivity of the engine oil. In our case $e=0.109\text{mm}$ (see Keita et al., 2014) and $\lambda=0.13\text{W/mK}$. From equation (4) we obtain the convection coefficient of engine oil hoilbearing which is equal to h_{crankpin} in our case.

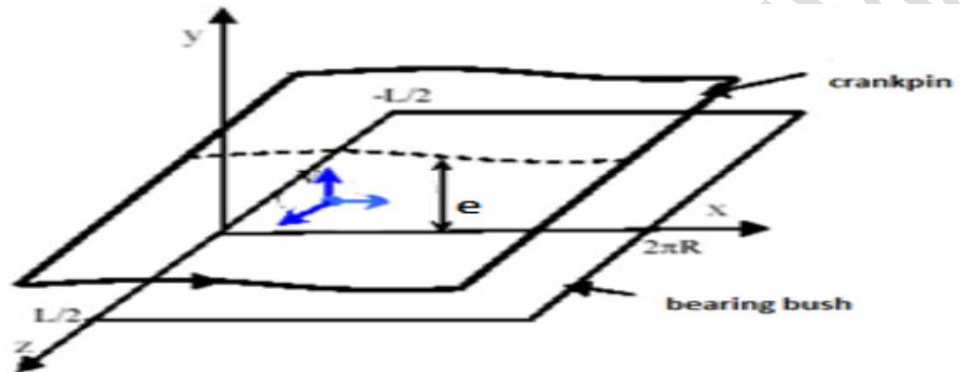


Figure 1. calculation scheme for convection coefficients (Jean, 1995)

3. RESULTS AND DISCUSSION

3.1. EXPERIMENTAL TEST AND RESULTS

Among the experimental results we are interesting to the maximum power engine (2650 tr/mm) and the maximum torque (1400 tr/mm) (Keita et al., 2014). In order to perform thermo-mechanical analysis, in this present study, the engine oil temperature have been measured

experimentally at the above two regimes. The values are: $99.8\text{ }^{\circ}\text{C}$ for the regime of maximum power and $90.3\text{ }^{\circ}\text{C}$ for the regime of maximum torque. The engine oil-crankshaft interaction under dynamic loading is studied on those different regimes numerically by the finite element method.

3.2. NUMERICAL SIMULATION RESULTS

In this section, we investigate crankshaft thermomechanical response by FEM for two types of analysis:

permanent and dynamic regime using numerical simulations. Figure 2 gives the crankshaft mesh and applied loads. The details of

calculation of these loads can be found in (see Keita et al., 2014).

Table 1 gives the parameters used in numerical simulations.

Table 1. Crankshaft Thermal and Mechanical properties

| Material | E (N/mm ²) | ν (-) | ρ (Kg/m ³) | Cp (J/KgK) | Hair (W/m ² K) |
|----------|---------------------------|--------------|--------------------------------|---------------|------------------------------|
| 42CD4 | 200.000 | 0,3 | 7800 | 460 | 100 |

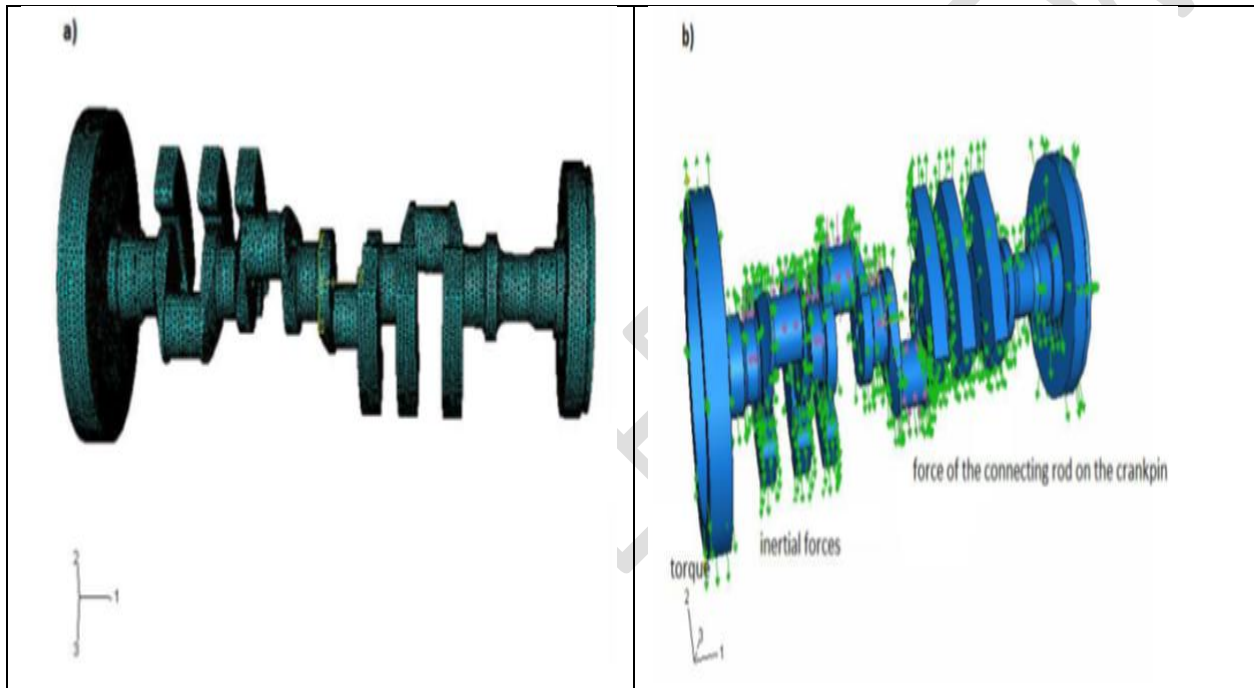


Figure 2. Crankshaft modelling: a) Mesh, b) applied loads

Among the numerical results from the simulations, we extract essentially the von Mises equivalent stress and temperature distribution inside the crankshaft.

3.3. Numerical results under permanent regime

There is a heat flow which enters on the crankshaft through crankshaft bearings and crankpins and, another one which comes out through the

flyweights and arms. This is because the crankcase air temperature is less than the engine oil temperature. In permanent regime, the equilibrium is reached when there is equality between the incoming flow through the bearings and crankpins and out coming flow by the flyweights and arms. Figure 3 shows the temperature distribution (Figure 3a) and the von Mises equivalent stress (Figure 3b) in

permanent regime. It can be observed (Figure 3a) that the maximum temperature is $90\text{ }^{\circ}\text{C}$ located on the crankpin 2. The Figure 4 illustrates the evolution of the temperature along the external surface of the crankshaft (crankpin, crankshaft bearing and arms) on the half crankshaft. As it can be seen the temperature level is most important on the crankpin and the crankshaft bearing respectively

compared to the arms. The minimum temperature on the arms is equal to $54.34\text{ }^{\circ}\text{C}$. The lowest temperature is recorded on the flyweights, $36.37\text{ }^{\circ}\text{C}$, this organ cools the crankshaft by ventilation effect. The thermal deformed is shown in Figure 5, the maximum principal deformation value is $1.23 \cdot 10^{-3}$ obtained on the central crankpin and crankshaft bearing.

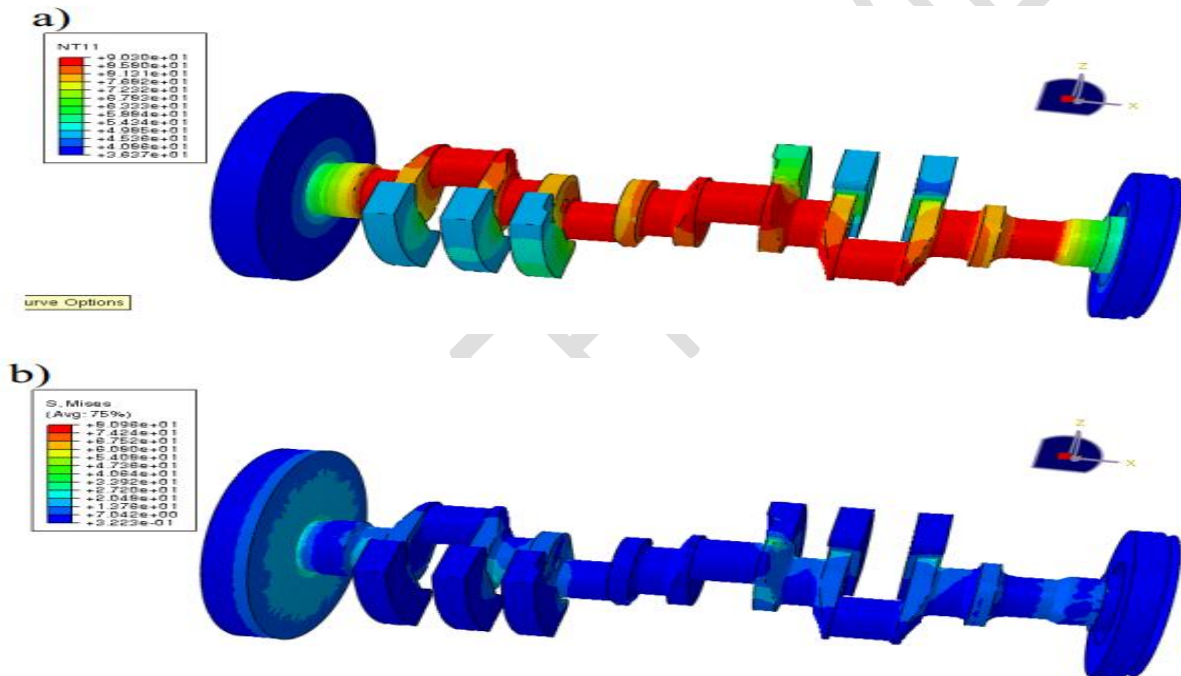


Figure 3. Numerical simulation results at permanent regime: a) temperature distribution, b) von Mises stress state

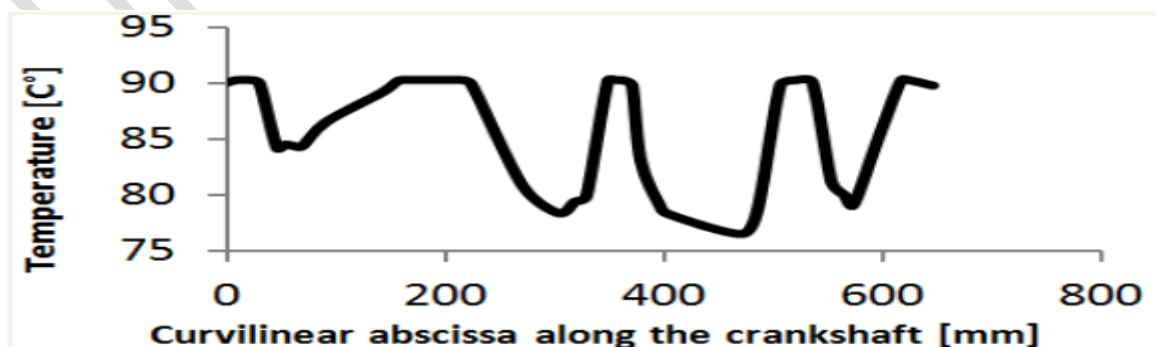


Figure 4. Evolution of the temperature along the external surface of the crankshaft

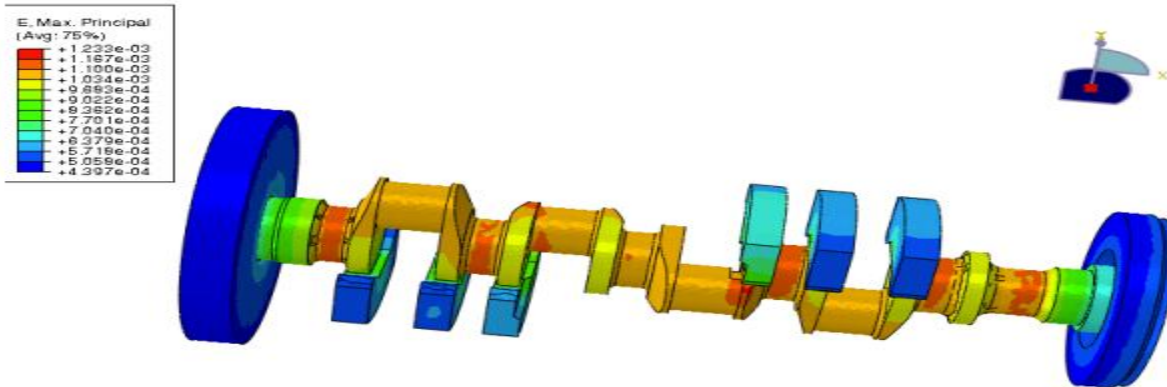


Figure 5. Equivalent principal strain state on the crankshaft

3.4. Numerical results under dynamic conditions

In this subsection the numerical results of the coupling of the crankshaft dynamic loading as defined in (Keita et al., 2014) to the thermal loading presented in the above sections is presented. The purpose is to analyse the influence of the dynamic loading on the thermal effects and to perform the thermo-mechanical fatigue study.

Figure 6 gives the comparison of the von Mises equivalent stress for permanent and dynamic regimes. It illustrates the influence of dynamic on the von Mises equivalent stress distribution inside the crankshaft at the end of the cycle. The maximum von Mises equivalent stress in dynamic simulation is 139.2 MPa located on the crankpin 2, while the maximum von Mises equivalent stress in permanent regime is 90.03 MPa.



Figure 6. von Mises equivalent stress: (a) permanent regime (b) dynamic regime at the end of the cycle

3.5. Thermo-mechanical fatigue analysis

The purpose of this subsection is to identify the thermomechanical fatigue resistance of the crankshaft in maximum engine loading conditions ($N = 2650 \text{tr/mn}$), which corresponds to the severe functioning state. The crankshaft is solicited by cyclic dynamic loads during its functioning inducing cyclic stresses. This situation leads to early damage (cracking or fracture), for a stress amplitude below the static tensile strength. The highest thermal stresses appear in areas where temperature gradients are highest (steady state). In this case, thermal stresses, superposed on the dynamic stresses will change the average stresses without changing the alternating stresses of dynamic loading. The thermo-mechanical fatigue will be addressed using the von Mises equivalent stress. For the fatigue analysis, we use the following Dang Van fatigue criterion.

3.5.1. Fatigue verification with Dang Van criterion

The Dang Van criterion is one of the multi-axial fatigue criteria. It predicts when the fatigue resistance limit of the material in N cycles is

reached under multi-axial stress state loading. This criterion is a global approach, it proposes a function using the amplitude $\tau_a(t)$ (alternating part) of octahedral shear stress and the hydrostatic pressure $p_H(t)$. This function is expressed as following (Bourauoi, 2007):

$$\max_n(\max_t\{[\tau_a(t)] + \alpha_D p_H(t)\}) \leq \beta_D \quad (5)$$

The alternative part $\tau_a(t)$ is expressed by the following equation:

$$\tau_a(\tau) = \tau(\tau) - \tau_m \quad (6)$$

Where $\tau(t)$ and τ_m are macroscopic octahedral shear stress and average split, respectively.

$\tau(t)$ is expressed in function of the stress tensor components:

$$\tau(t) = \frac{1}{3} \sqrt{(\sigma_1 - \sigma_2)^2 + (\sigma_2 - \sigma_3)^2 + (\sigma_3 - \sigma_1)^2} \quad (7)$$

While τ_m is defined as

$$\tau_m = \int_0^T \tau(x, y, z, t) dt \quad (8)$$

The constants α_D and β_D can be determined by the means of reference fatigue tests (Gazaudet al., 1969) (see details in Keita et al., 2014). By substituting equations (6-8) into equation (5) we can obtain the

following fatigue resistance condition:

$$\tau_a + 0,198P_{Hmax} \leq 294,3(9)$$

The Figure 7 gives the comparison between dynamic and thermo-mechanical under dynamic loading simulations of Dang van diagrams at crankpin 2 (most stressed zone). As it can be seen, in the thermo-mechanical under dynamic loading simulation, the point to be check (red point in Figure 7) is higher and closer to the endurance limit curve compared to the dynamic

simulation. This can be explained by the fact that in thermo-mechanical under dynamic loading simulation, thermal stresses is superposed on the dynamic stresses leading to the reduction of the safety coefficient regarding fatigue analysis. At the end we compare in Figure 8 the picture of crankshaft damage in service to the position of the most stressed zone obtained in numerical simulations. The comparison shows the breakage occurred in an area where the numerical simulations give highest stresses.

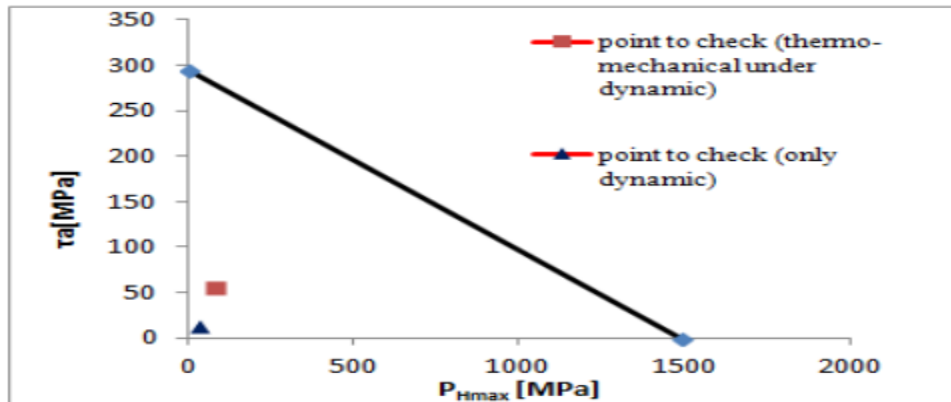


Figure 7. Fatigue verification at the crankpin 2. Dang van Diagram

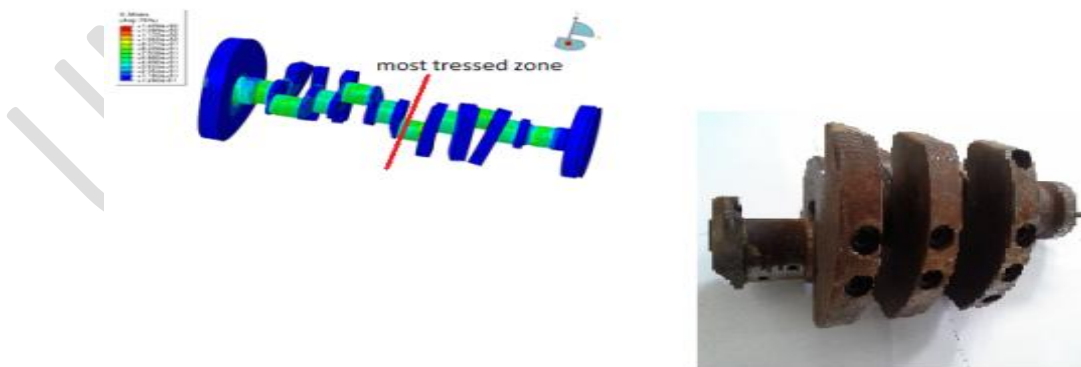


Figure 8. Comparison of crankshaft breakage in service to the numerical simulation results

4. CONCLUSIONS

This paper has enabled to develop a numerical model account of the thermal effects coming from the engine-oil-crankshaft interaction modelling. This thermomechanical behavior have been investigate under severe dynamic conditions. As case of application, the crankshaft of a diesel engine air cooled was considered. As boundary conditions, the heat convective flux of the engine oil and crankcase air have been considered in interaction with the crankshaft. FEM simulations have allowed to compute the stress fields of thermomechanical origin, leading to the identification of the most

solicited zones which are the risk zones. To validate the thermo-mechanical endurance under dynamic loading, an analysis of the thermo-mechanical fatigue resistance was carried out in these zones using Dang Van multi-axial fatigue criterion, which takes into account the multiaxial cyclic loading of crankshaft. To prove our model efficiency we compared crankshaft damage in service to the numerical simulations results. It was found the breakage occurred in an area where the numerical simulations give the highest stresses.

REFERENCES

1. Atkinson, B., Brocklebank, M.P., Card, C.C.H and Smith, J.M. (1969). Low Reynolds number Developing flows. AICHE J. 15, P, p. 548-53.
2. Bouraoui, C., Fathallah, R., Khantouch, Z., Alaah. Châteauneuf, A. and Destrebeq, J.F. (2007). Analyse comparative des critères de fatigue multiaxiale basée sur une approche fiabiliste: étude de cas. Congrès CMSM 2007. Monastir, Tunisie.
3. Caton, J.A. and Heywood, J.B. (1981). An Experimental and Analytical study of heat transfer in an Engine exhaust port. Int. J. Heat Mass Transfer. Vol. 24, No. 4, pp. 581-595, 1981.
4. Gazaud, R., Pomey, G., Rabbe, P. and Janssen, CH. (1969). La fatigue des métaux. DUNOD. Paris.
5. Huetz, J. and Petit, J.P. (1990). Techniques de l'Ingénieur. Génie énergétique, vol. 1, N° A1540, Paris, France.
6. Jean, F. (1995). Butées et Paliers hydrodynamique. Techniques de l'ingénieur. B-5320.
7. Keita, O., Bessrou, J., and Tahar, H. (2014). A Model for Dynamic behavior of the Crankshaft of an air Cooled Diesel Engine Subjected to Severe Functioning. Int. J.

- Automotive Technology Vol. % 15, %No. %5, %pp. %823833.
8. Meng, J., Liu, Y. and Liu, R. (2011). Finite Element Analysis of 4-Cylinder Diesel crankshaft. In. J. Image, Graphics and Signal Processing, 2011, 5, 22-29.
 9. Metkar, R.M., Sunnapwa, V.K. and Hiwas, S.D. (2011). A Fatigue Analysis and Life Estimation of Crankshaft-A Review. Int. J. Mechanical and Materials Engineering. Vol.6, No.3, 425-30.
 10. Mourelatos, Z. P. (2001) A crankshaft system model for structural dynamic analysis of internal combustion engines. Combustion and engines, vol. 79pp. 2009-2027
 11. Niccoli, F., Maletta, C., Sgambitterra, E., and Furgiuele, F. (2015). A Thermo-mechanical Model for Shape Memory alloy-based Crank heat Engines. Journal of Intelligent Material Systems and Structures. vol. 26, 6, pp. 652-662.
 12. Niinoa, T., Iwamoto, T. and Ueda, S. (2002). Development of simulation technology for dynamic behavior of crankshaft systems in motorcycle engines. JSAE Review 23, 2002, -127-131.
 13. Patil, S., Sollapur, S., Pawar, V., and Wange, S. (2015). Thermo-Mechanical Analysis of Crankcase. IOSR. J. of Mechanical and Civil Engineering. Volume 12, Issue 5 Ver. V (Sep. - Oct. 2015), PP 13-18.
 14. Taher, H. (2003). Un modèle thermomécanique d'un moteur à combustion interne refroidi par air. Mémoire de DEA. ENIT.
 15. Woschni, G. (1967). A universally applicable equation for the instantaneous heat transfer coefficient in the internal combustion engine. SAE Paper No 670931, 1967.